Limited and strain-specific transcriptional and growth responses to acquisition of a multidrug resistance plasmid in genetically diverse *Escherichia coli* lineages

Steven J. Dunn*[1], Laura Carrilero*[2], Michael Brockhurst[2], Alan McNally[1]

*Joint first authors contributed equally

[1]Institute of Microbiology and Infection, College of Medical and Dental Science, University of Birmingham, Birmingham B15 2TT

[2]Division of Evolution and Genomic Sciences, School of Biological Sciences, University of Manchester, Manchester M13 9PT

Running title: Transcriptional response to MDR plasmids in *E. coli*

Abstract

Multi-drug resistant (MDR) *Escherichia coli* are a major global threat to human health, wherein multi-drug resistance is primarily spread by MDR plasmid acquisition. MDR plasmids are not widely distributed across the entire *E. coli* species, but instead are concentrated in a small number of clones. Here, we test if diverse *E. coli* strains vary in their ability to acquire and maintain MDR plasmids, and if this relates to their transcriptional response following plasmid acquisition. We used strains from across the diversity of *E. coli*, including the common MDR lineage ST131, and the IncF plasmid, pLL35, encoding multiple antibiotic resistance genes. Strains varied in their ability to acquire pLL35 by conjugation, but all were able to stably maintain the plasmid. The effects of pLL35 acquisition on cefotaxime resistance and growth also varied among strains, with growth responses ranging from a small decrease to a small increase in growth of the plasmid-carrier relative to the parental strain. Transcriptional responses to pLL35 acquisition were limited in scale and highly strain specific. We observed significant transcriptional responses at the operon or regulon level, possibly due to stress responses or interactions with resident MGEs. Subtle transcriptional responses consistent across all strains were observed affecting functions, such as anaerobic metabolism, previously shown to be under negative frequency dependent selection in MDR *E. coli*. Overall there was no correlation between the magnitude of the transcriptional and growth responses across strains. Together these data suggest that fitness costs arising from transcriptional disruption are unlikely to act as a barrier to MDR plasmid dissemination in *E. coli*.

38 **Importance**

39 Plasmids play a key role in bacterial evolution by transferring niche adaptive functions
40 between lineages, including driving the spread of antibiotic resistance genes. Fitness
41 costs of plasmid acquisition arising from the disruption of cellular processes could limit
42 the spread of multidrug resistance plasmids. However, the impacts of plasmid
43 acquisition are typically measured in lab-adapted strains rather than in more
44 ecologically relevant natural isolates. Using a clinical multidrug resistance plasmid and
45 a diverse collection of *E. coli* strains isolated from clinical infections and natural
46 environments, we show that plasmid acquisition had only limited and highly strain-
47 specific effects on bacterial growth and transcription. These findings suggest that
48 fitness costs arising from transcriptional disruption are unlikely to act as a barrier to
49 plasmid transmission in natural populations of *E. coli*.

50

Introduction

Multi-drug resistant (MDR) *Escherichia coli* present a global public health risk and are listed by the World Health Organisation as a priority pathogen. The incidence of MDR *E. coli* as aetiological agents of human disease has steadily increased since the turn of the century (Mathers et al., 2015). Initially this was due to the emergence of *E. coli* clones carrying plasmids containing extended spectrum beta-lactamase (ESBL) genes conferring resistance to third generation cephalosporins (Mathers et al., 2015). This emergence mirrored the rise in the incidence of *E. coli* as the causative agent of bloodstream infections world-wide, primarily due to the rapid global dissemination of MDR clones (Banerjee & Johnson, 2014; Mathers et al., 2015). This was followed by the emergence of clones carrying plasmids containing carbapenemase enzyme genes, conferring strains resistance to all antimicrobial classes with the exception of colistin (Peirano et al., 2011; Wu et al., 2019).

The emergence of MDR *E. coli* has not occurred evenly across the species. Rather MDR plasmid carriage is concentrated in a number of clones associated with extra-intestinal infections, whilst it is rarely seen in clones causing intestinal infectious disease or in exclusively commensal lineages (Dunn et al., 2019). ESBL plasmid carriage is most commonly seen in low-diversity clones of lineages such as ST131, ST648, and ST410 (Dunn et al., 2019), with ST131 representing the most common cause of MDR *E. coli* bloodstream and urine infections in the developed world (Banerjee & Johnson, 2014). Carriage of carbapenemase plasmids is also concentrated in low-diversity clones of lineages such as ST167 and ST410, both of which belong to the Phylogroup A clade of *E. coli* which are generally devoid of most common *E. coli* virulence factors (Feng et al., 2019; Wu et al., 2019; Zong et al., 2018).

Comparison of the genomes of MDR plasmid carrying clones with the lineages that those clones emerged from shows striking similarity in key steps in their evolution. All show rapid clonal expansion of MDR plasmid carrying strains which are globally distributed in a matter of years (Feng et al., 2019; Petty et al., 2014; Zong et al., 2018). The MDR clones also carry clone specific alleles of key genes encoding traits involved in human colonisation, such as adhesins and iron acquisition (Feng et al., 2019; McNally et al., 2019; Zong et al., 2018). Comprehensive analysis of ST131 MDR clade C showed it differed from the drug susceptible clade A and B of the lineage in a number of unique alleles of genes involved in colonisation as well as anaerobic metabolism genes (McNally et al., 2019). MDR clones also contain unique intergenic-sequence alleles, which correlate with plasmids carried by strains (McNally et al., 2016)(Feng et al., 2019; Zong et al., 2018).

As well as the biosynthetic burden associated with replicating, transcribing and translating the new genetic material, plasmid acquisition often disrupts cellular homeostasis. For example, large-scale changes to regulation of chromosomal genes have been observed following plasmid acquisition in a range of bacterial hosts (Harrison et al., 2015; Millan et al., 2015; San Millan et al., 2018), which can be negated by compensatory mutations to regulators. The shared genetic traits of MDR clones of *E. coli* including regulatory sequences together with the uneven distribution of MDR plasmids, suggests that some lineages of *E. coli* may be better preadapted to the acquisition and stable integration of MDR plasmids than others, potentially suffering less cellular disruption (Dunn et al., 2019; McNally et al., 2016). However, data comparing the transcriptional and phenotypic responses of diverse *E. coli* strains to MDR plasmid acquisition are lacking.

We tested the transcriptional response to acquisition of an ESBL plasmid encoding CTX-M-15 and TEM-112 in eight genetically diverse *E. coli* strains, including environmental *E. coli* isolates from lineages in which MDR plasmids have never been reported, and strains from clade A, B and C of *E. coli* ST131, wherein clade C is most frequently associated with MDR plasmid acquisition. Strains varied in the rate of ESBL plasmid acquisition by conjugation from *K. pneumoniae* and the degree of cefotaxime resistance conferred by the plasmid but not in stability of the plasmid once acquired. ESBL plasmid carriers showed variations in growth relative to plasmid free cells ranging from impaired to enhanced relative growth of ESBL plasmid carriers. Plasmid transcription did not vary significantly among host strains, but we observed strain specific differences in chromosomal gene expression caused by plasmid acquisition. We observed no correlation between the degree of transcriptional disruption caused by plasmid acquisition and the relative growth of ESBL plasmid carriers.

Materials and Methods

Bacterial strains and plasmids

A total of 8 *E. coli* strains were selected for use in this study, representing sequence types 131 (clades A, B, and C), 394, and 1122 (Table S1). All strains were screened to ensure that they did not contain any existing MDR plasmids. This study used plasmid donor strain LL35 (a *Klebsiella pneumoniae* isolate belonging to ST-45) which contains pLL35, a 106 kb incFII(K)-9 plasmid with a complete conjugative transfer machinery, and a complex antibiotic resistance region (Figure S1). The resistance region in pLL35 is comprised of multiple translocatable genetic elements. It contains several complete antibiotic resistance genes, conferring resistance to cephalosporins

and beta-lactams (*blaCTX-M-15*, *blaTEM-112*), aminoglycosides (*aacA4, aacC2, aadA1*) and quinolones (*qnrS1*). This region also contains OXA-9, however this gene is truncated due to a premature stop codon. The antibiotic resistance region is potentially mobilizable, due to an ISEcp1 insertion sequence. pLL35 also encodes two separate toxin/antitoxin systems (*higAB*, *ccdAB*).

Plasmid conjugation

Twelve independent conjugation assays were performed for each strain. A single colony from overnight growth on nutrient agar was inoculated into 5 ml of nutrient broth (Oxoid, UK). This was incubated at 37˚C for 2 hours with shaking (180 rpm). Cultures were mixed at a ratio of 1:3 donor to recipient and 50 µl were used to inoculate 6 ml of BHI. Six replicates were incubated as static cultures at 37˚C for 24 hours, and six replicates were incubated as shaken cultures at 37˚C for 24 hours at 180 rpm.

The conjugation mix was plated onto UTI Chromagar (Sigma Aldrich, UK) supplemented with 4 µg/ml of cefotaxime and incubated at 37˚C overnight. Colonies that produced a phenotype indicative of *E. coli* were further subcultured onto UTI Chromagar with 4 µg/ml of cefotaxime in order to check the resistance profile, and to ensure there was sufficient pure growth to store for subsequent use. One of these replicates was used to quantify differential gene expression and is subsequently referred to as the transconjugant. Whole genome sequencing (WGS) data was also generated for three additional replicates from the conjugation assays, which are referred to as the transconjugant replicates.

In the generation of conjugated strains, bacteria were sub-cultured a total of 5 times. In order to account for any basal adaptation to the lab conditions, and to control for any variation generated by variables extraneous to the plasmid conjugation, the parental recipient strains were also run through the conjugation protocol with a plasmid free *Klebsiella* strain Ecl8 (Buckner et al., 2018). These triplicate samples were also sequenced and are referred to as the control replicates.

Genome sequencing

Whole genome sequencing was performed on the ancestral, transconjugant, control replicates and transconjugant replicate strains. The ancestral and transconjugant lines were sequenced by both Illumina and Oxford Nanopore based technologies. Illumina sequencing was provided by MicrobesNG (http://www.microbesng.com). Illumina genome sequence reads were assessed for quality using FastQC (V 0.11.9), and subsequently trimmed using Trimmomatic (V 0.3)14 with a sliding window quality of Q15 and length of 20 base pairs. Kraken (V 2) was used to confirm species ID and check for potential contaminants.

Long read sequencing was performed on DNA extracted using a phenol/chloroform method. DNA was quantified using the Qubit 4.0 and a broad range dsDNA kit (ThermoFisher, UK). Libraries were prepared using the SQK-LSK109 sequencing kit, and EXP-NBD104 expansion set. The libraries were then sequenced on a MinION rev 4.1D using a R9.1 flowcell over 48 hours (Oxford Nanopore Technologies, UK).MinION data was basecalled using GPU-accelerated Guppy (V 3.1.5+781ed57) in high accuracy mode. Adapters were confirmed and removed using Porechop (V 0.2.3_seqan2.1.1). Reads that had differential demultiplexing via Guppy and

Porechop were discarded, leaving only reads for which both programs had reached a consensus. Chimeric reads were discarded using Unicycler's Scrub module (V 0.4.7). Finally, reads were filtered using FiltLong (V 0.2.0), with parameters based on read length and quality distributions generated by NanoPlot (V 1.24.0), removing relatively short or low-quality reads (e.g. lower 10% of the distribution).

Circularised assemblies were produced using both the long and short read data by Unicycler (V 0.4.7) (Wick et al., 2017). Following assembly, we ran additional rounds of Pilon (V 1.23) until no further changes were found. Assemblies were annotated using Prokka (V 1.13.3) (Seemann, 2014). Structural variants were identified using a combination of Sniffles (V 1.0.12) and Assemblytics (V 1.0). Structural variants were further filtered to high confidence calls by inspecting the BAM file and filtering to discard minor allele variants (AF <0.9). Single nucleotide variants were called against the hybrid assemblies using Snippy (V 4.3.6).

Transcriptome sequencing

RNA sequencing was performed on biological triplicates of the ancestral and transconjugant strains. For each replicate, a colony was picked from overnight growth on Nutrient Agar and added to 5 ml of Nutrient Broth (Sigma Aldritch, UK). Cultures were incubated at 37˚C until reaching an OD600 of ~0.6. RNA was extracted using Trizol (ThermoFisher, UK). Following isopropanol precipitation, DNA was digested using Turbo DNAse (Thermofisher, UK) based on the manufacturer's protocol. The final RNA solution was purified using a RNeasy Mini Kit (Qiagen, UK), and quantified using a Qubit with the RNA HS assay kit. The RNA was immediately stored at -80˚C.

RNA sequencing was performed by the Centre for Genomics Research (Liverpool, UK). The RNA integrity number and library insert size were verified using the Agilent RNA 6000 Pico Kit and Bioanalyzer platform (Agilent, USA). The RiboZero (Illumina, USA) kit was used to deplete rRNA, and dual indexed libraries were prepared using the NEBNext Ultra Directional RNA sequencing kit (New England Biolabs, USA). Libraries were sequenced on a HiSeq 4000 (Illumina, USA) configured to 2 x 150 bp cycles. In order to obtain at least 10 million reads per sample, the sequencing run was distributed across three lanes.

Kallisto (v 0.46.0) was used to quantify differential gene expression, with the high-quality hybrid *de novo* assemblies of parental strains used as a reference. Input files were prepared using Prokka (v 1.13.3) for annotation, genbank_to_kallisto.py (https://github.com/AnnaSyme/genbank_to_kallisto.py) to convert the annotation files for use with Kallisto, and GNU-Parallel (v 20180922) for job parallelisation. Differential gene expression was analysed using Voom/Limma in Degust (V 3.20), with further processing of the resulting differential counts in R (V 3.5.3). UPGMA clustering was performed using DendroUPGMA (http://genomes.urv.cat/UPGMA/). Functional categories were assigned to genes using eggnog-mapper (V 2).

Plasmid persistence

To determine the persistence of the plasmid over time, 4 replicate cultures of each plasmid-containing strain were propagated by daily serial transfer in nutrient broth (NB) microcosms (6 ml of NB in a 30 ml glass universal) for 16 days. 1% of each culture was transferred to fresh media every 24 hours. Populations were plated out onto nutrient agar ± 4μg/ml of cefotaxime at days 0, 1, 2, 4, 7, 10, 13 and 16.

225 **Growth curves and phenotypic profiling**

226 Minimum inhibitory concentration (MIC) assays for the ancestral and transconjugant
227 strains were conducted according to the CLSI guidelines (CLSI, 2012), using nutrient
228 broth and cefotaxime. Briefly, assays were performed in 96 well plates at final
229 cefotaxime concentrations of 0.25, 0.5, 0.75, 1, 1.25, 1.5, 1.75, and thereafter two-fold
230 increases from 2 to 2,048 µg/ml.

231

232 Growth kinetics for both plasmid-free and plasmid-containing strains were measured
233 using cultures grown in 200 µl nutrient broth per well in a 96 well plate using an
234 automated absorbance plate reader (Tecan Spark 10). Wells were inoculated using
235 the same procedure described above. Plates were incubated at 37 °C for 39 hours
236 and the optical density of each well was measured every 30 minutes at 600 nm, plates
237 were shaken for 5s (orbital shaking, movement amplitude 3mm, 180 rpm) and allowed
238 to settle for 50s prior to each reading. A humidity cassette was used to minimise
239 evaporation of the samples.

240

241 **Data availability**

242 Sequence data is available under bioproject PRJNA667580, and individual SRA
243 accessions are provided in Table S1.

244

245 **Results**

246

247 ***E. coli* strains varied in conjugational uptake of an ESBL plasmid**

248 For most strains, the conjugation rate from *K. pneumoniae* was higher in static than in
249 shaken culture. Indeed, for several strains we detected no transconjugants from

shaken cultures in any of the replicates (e.g., F022 and F047 – ST131 clade A and C, respectively), and only three strains consistently acquired the plasmid in both shaken and static conditions (i.e., F037, F048, F054 – all ST131 clade B/C – Figure S1). Due to the high number of missing replicates in shaken cultures, we were only able to analyse variation across all strains in the conjugation rates estimated from static cultures. In static cultures, strains varied in their ability to acquire the plasmid by conjugation from *K. pneumoniae* (Figure S2; ANOVA, strain effect, $F_{7,36}$ = 19.23 P = 2.06e-10). Once acquired, however, the plasmid was stably maintained over time by all strains (Figure S3; Wilcoxon test comparing population density averaged over time on media with or without cefotaxime, all strains, P > 0.05).

Strain-specific effects of ESBL plasmid carriage on resistance and bacterial growth kinetics

Plasmid acquisition increased resistance to cefotaxime but the level of resistance conferred by the plasmid varied by strain (Figure 1; ANOVA, strain by plasmid interaction, $F_{7, 32}$ = 2.968, P = 0.0163). Specifically, in strains F037, F047 and F054 the plasmid provided lower levels of cefotaxime resistance than in plasmid bearers of the other strains.

Parental strains varied in their growth parameters (lag time, ANOVA, $F_{7, 32}$ = 5.358, P = 0.000394; maximum growth rate, ANOVA, $F_{7, 32}$ = 6.3, P = 0.000108; saturation density, ANOVA, $F_{7, 32}$ = 18.48, P = 0.00000000136; integral of the growth curve, Kruskal-Wallis X^2_7 = 31.759, P = 0.000045). To control for this variation in baseline growth among the strains, we normalised growth parameters per plasmid-carrying strain by its corresponding parental strain. This gave estimates of relative growth

parameters, and thus of the impact of plasmid acquisition upon the growth of each strain (i.e., a value of 1 would indicate no effect on growth of plasmid acquisition; Figure 2). Strains varied in their relative maximum growth rate (ANOVA, $F_{7, 32} = 5.742$, $P = 0.00023$), relative saturation density (Kruskal-Wallis ${}_X{}^2{}_7 = 24.102$, $P = 0.001093$), and relative integral of the growth curve (ANOVA, $F_{7, 32} = 8.998$, $P = 0.00000424$), but not in their relative lag time (Kruskal-Wallis ${}_X{}^2{}_7 = 10.264$, $P = 0.1741$). The clearest impacts of plasmid acquisition on growth were apparent for the relative integral of the growth curve (Figure 2), which is a useful measure of the overall effect of plasmid acquisition on growth (Wright et al., 2018): The integral of the growth curve was reduced by plasmid carriage in the strains GU15 and F047 (one-sample t-test of relative integral against 1; GU15, $t = 3.6933$, $df = 4$, $P = 0.021$; F047, $t = 4.1762$, $P = 0.014$) but was increased in the strains F022 and F037 (one-sample t-test of relative integral against 1; F022, $t = 7.0987$ $df = 4$ $P = 0.0021$; F037, $t = 5.0836$, $P = 0.0071$). Thus, acquiring the ESBL plasmid had variable effects upon growth across the strains causing both increased and decreased growth, whilst having a negligible impact upon the growth of half of the strains tested.

Following the masking of any variants that occurred in the ancestral or control sequence data, ESBL plasmid carriers contained very few SNPs, with the majority of isolates containing no SNPs at all (n=6 out of 8). The position of detected SNPs was determined, but no clear evidence of parallelism could be established (Table S2). To confirm this limited genomic impact further, we sequenced three additional independently constructed transconjugant replicates. This also revealed a small number of SNPs (0-2 SNPs per replicate), with the majority of sequences containing 0 variants (n=16 out of 24).

300

301 **Strain specific transcriptional responses to acquisition of an ESBL plasmid**

302 We next compared the transcriptomes of the pLL35 carrying transconjugants with their
303 parental strain to determine the effect of ESBL plasmid acquisition on host gene
304 expression. Combining differential gene expression analysis from three independent
305 biological replicates showed very little significant transcriptional response in any strain,
306 with the number of significantly 2-fold differentially expressed genes ranging from 22
307 to zero at a false discovery rate (FDR) P-value of < 0.05 and 31 to zero at a FDR P-
308 value of < 0.1 (Figure S3). Volcano plots for the transcriptional impact of ESBL plasmid
309 acquisition per strain show highly strain-specific responses to acquisition of the ESBL
310 plasmid, both in terms of the level of transcriptional response and the genes that were
311 differentially expressed (Figure 3). Strains ELU39, F104 and F037 showed no
312 significant changes in gene expression upon acquisition of the plasmid (at FDR P-
313 value of < 0.05 or < 0.1), strains GU15, F054 and F048 had fewer than 5 genes
314 significantly differentially expressed, and strains F022 and F047 showed between 10
315 and 22 genes significantly differentially expressed (at FDR P-value of < 0.05, Figure
316 S4). There was no correlation between magnitude of transcriptional response and the
317 growth responses observed in the strains ($r = -0.6162$, $P = 0.1038$).

318

319 **Functions whose expression was affected by ESBL plasmid acquisition varied**
320 **between strains**

321 We observed differences in the functions whose expression was significantly affected
322 by ESBL plasmid acquisition between the strains. In F022 plasmid-carriers we
323 observed upregulation of the entire class 1, 2 and 3, flagella biosynthesis regulons
324 relative to the plasmid-free parental strain (Chilcott & Hughes, 2000). Further

inspection of the genome sequences of the parental and transconjugant F022 strains revealed that this occurred due to an insertion of an IS1 family IS element in *lrhA,* the negative regulator of *flhDC* (Figure 4).

In F047 the ESBL plasmid caused upregulation of a variety of chromosomal genes, including those involved in various stress responses such as *cpxP* (envelope stress response), *deaD* (low temperature response), *ibpAB* (heat and oxidative stress), and *soxS* (superoxide stress master regulator). This is mirrored in several differentially expressed genes just below the 2 log fold change significance threshold such as *dnaJ, degP* and *osmY* (1.81, 1.64 1.59 FC), which are all involved in stress response. The presence of plasmid also led to upregulation of *marR*, the repressor of the *mar* antibiotic resistance and oxidative stress response regulon, though *marA* expression was not significantly affected (1.0 FC, 0.57 FDR). Other functions upregulated by plasmid acquisition included metabolic transport (*mgtA, pstS*) and anaerobic metabolism genes (*glpD*).

In F048, several co-located hypothetical genes were upregulated, 3 of these were significantly upregulated while the remainder were slightly below the FDR significance threshold. This region was further characterised with Prophage Hunter, showing a putative ~60 Kb prophage. This prophage contains 78 genes and shows 94% identity and 28% coverage with prophage CUS-3. No evidence of phage mobilisation was detected by structural variant analysis, and the read depth at this region (normalised to house-keeping genes) was consistent across both the parental and transconjugant read sets suggesting that the observed upregulation was not due to the presence of additional prophage copies.

In GU15 the ESBL plasmid led to down regulation of the entire sulfur biosynthesis and transport operons (*cysA – cysW*). Significant downregulation was observed in *cysA* at FDR >0.05, and *genes cysHIJKNWU* at FDR >0.1. The rest of the operon were expressed at ranges slightly below the FDR significance threshold.

Consistent pattern of low-level transcriptional response to acquisition of the ESBL plasmid

Some genes known to be in operons or regulons did not pass significance threshold in our FDR analysis, despite the rest of the operon or regulon doing so. This is due to our use of amalgamated data from three independent biological replicates and strict significance thresholds. We decided to further analyse the expression of all core genes (Figure S5) using a principal component analysis to detect genes that were differentially expressed across our host range (Figure S6). Analysis of this set of genes showed some consistent patterns of differential expression across all strains. A common pattern of upregulation in response to acquisition of the ESBL plasmid was observed for the *cit* operon, *his* operon, the *hya, hyb,* and *hyc* operon, and the *nar* and *ttd* operons and the *gad* loci (Figure 5). Conversely, there was a common pattern of down-regulation in response to acquisition of the ESBL plasmid of the *csg, gat, waa, yad,* and *yih* operons across all strains. Functional enrichment analysis of genes in the 5th and 95th percentile of these differentially expressed loci confirmed this consistent fine-scale transcriptional response to the plasmid in genes associated with the cell wall, signal transduction, cell motility, energy production and conversion, and carbohydrate transport and metabolism (Figure 5).

Discussion

Evidence from experimental evolution studies has provided us with a detailed picture of the impact that acquisition of plasmids and their stable integration into a host cells genetic inventory has on cell fitness (Brockhurst et al., 2019). Much of this fitness impact is driven by changes in transcription in the acquiring cell, both the need to transcribe genes on the plasmid, but also global effects on host cell transcription to offset the impact of carrying the plasmid (Buckner et al., 2018; Harrison et al., 2015; Millan et al., 2015). There are very few of these studies examining the impact of acquisition of multi-drug resistance plasmids on cells from genetically diverse strains (Buckner et al., 2018), with most evidence of adaptations that occur as a result of MDR plasmid acquisition stemming from large comparative population genomics studies (Feng et al., 2019; McNally et al., 2016, 2019). Here we address this by examining the impact of acquisition of an MDR plasmid on *E. coli* from a variety of genetic backgrounds ranging from environmental lineages with no reported MDR plasmid carriage to MDR-plasmid-free clinical isolates from the ST131 lineage most commonly associated with multi-drug resistance in clinical settings.

Acquisition of the ESBL plasmid varied among strains, although all strains stably maintained the plasmid once they had acquired it, likely due to the presence of two toxin-antitoxin systems on pLL35. Plasmid acquisition had variable effects on growth between strains. Notably, plasmid acquisition was not costly in terms of relative growth for all the strains, with increased growth of plasmid carriers relative to their parentals observed in two strains. This is surprising given that plasmid acquisition has been shown to be associated with fitness costs across a diversity of plasmid-host interactions, although variation in the magnitude of the cost has been described

(Bouma & Lenski, 1988; Göttig et al., 2016; Kottara et al., 2018; Nang et al., 2018). However, our data are consistent with those of another recent study that tested the fitness effect of a given plasmid across the range of genetic backgrounds present in a host species. Like ours this study reveal diverse fitness impacts ranging across a continuum from costly to beneficial (Alonso-del Valle et al., 2020). These data highlight that the fitness effects of a plasmid can be highly strain-specific, and thus are likely to arise from specific genetic interactions rather than the generic biosynthetic costs of plasmid maintenance. Interestingly, effects on growth of plasmid acquisition were uncorrelated with the extent of changes in gene expression across the strains, suggesting that greater plasmid-mediated gene dysregulation does not necessarily translate to larger fitness costs.

Strains varied in the level of cefotaxime resistance provided by the ESBL plasmid. This suggests epistasis between the plasmid ESBL gene and chromosomal loci that vary among strains. Through comparison of the strain genomes we could not identify any clear differences in chromosomal gene content among strains in terms of known resistance determinants to explain the observed variation in cefotaxime resistance. For example, all strains encode the same set of standard efflux pumps with the exception of F047 and F048, which also contain *tetA*. Yet F047 and F048 differ markedly to each other in their cefotaxime resistance response, suggesting that TetA does not explain the variable resistance response. All strains encode a variant of *blaEC*. In addition, F022 and F047 encode *blaTEM-1* but vary in their cefotaxime resistance response, suggesting that *blaTEM-1* does not explain the variable resistance response. This is perhaps unsurprising as the prediction of a strain's

resistance phenotype from gene content alone is notoriously inaccurate (Mahfouz et al., 2020).

Comparing the transcriptomes of plasmid-carriers with their parental strain revealed highly strain-specific effects of plasmid acquisition on the expression of chromosomal genes. The number of genes whose transcription was affected by the plasmid was small in all strains, ranging from 0 to just 22 genes (at FDR < 0.05). These data stand in contrast to other studies where the expression levels of hundreds of chromosomal genes are affected by plasmid acquisition (Harrison et al., 2015; Long et al., 2019; Millan et al., 2015; Takahashi et al., 2015). Significant transcriptional effects of ESBL plasmid acquisition were focussed in discrete operons or regulons. For example, in GU15 we observed down-regulation of the sulfur biosynthesis and transport operons (*cysA* – *cysW*). In F048 plasmid-carriers, flavohaemoglobin (Hmp), which is responsible for resistance to nitrosative stress (Stevanin et al., 2007), was upregulated following plasmid acquisition. In F047, the transcriptional impact of plasmid acquisition was more widespread, affecting more diverse functions, but, consistent with F048, most of these were related to stress-responses. Upregulation was observed in *marR*, which did not extend to *marA*; *marA* has been demonstrated to have a short half-life (3 minutes) and is quickly depleted when the environmental stress is removed (Vinué et al., 2013). Increased expression was also observed in heat shock proteins IbpA/B. The function of IbpA/B extends beyond heat stress; previous studies have shown that increased *ibpA/B* expression resulted in the overproduction of a beta-lactamase precursor, potentially through IbpA/B binding to the precursor protein, preventing subsequent processing (Kuczyńska-Wiśnik et al., 2002). This could explain the lowered cefotaxime MIC observed, though the exact cause of *ibpA/B* upregulation is

449 unclear. All of these factors indicate that F047 exhibited a strong stress response to
450 acquisition of the plasmid. Plasmids are known to elicit stress responses in their host
451 cells (San Millan et al., 2018), for example through the conjugation-mediated cell
452 envelope stress in *E. coli* (Yang et al., 2008). It is hypothesised the production of
453 conjugation apparatus may lead to misfolded proteins; F047 failed to conjugate in
454 shaking conditions. This may be due to an increase in the concentration of damaged
455 or misfolded proteins beyond that which would be mitigated by increased expression
456 of stress response proteins (e.g. DegP, CpxP).
457
458 In two of our strains there is evidence of a transcriptional response possibly driven by
459 the relationship between mobile genetic elements. In F022, the upregulation of
460 flagellar and chemotaxis genes was explained by a 768 bp insertion of an IS1 family
461 element encoding both *insA* and *insB* in the *lrhA* regulator. LrhA belongs to the lysR
462 family and binds to and negatively regulates expression of the *flhDC* master regulator.
463 Truncation of *lrhA* is therefore likely to have prevented negative regulation of *flhDC*,
464 leading to uncontrolled expression of the flagellar and chemotaxis operons. Genomic
465 comparison of IS elements within the F022 genome revealed 7 identical IS1
466 sequences in the parental genome, with 4 found on the chromosome, and 3 on a
467 canonical plasmid. Upon plasmid acquisition, this element inserted one additional
468 time. This appeared to be a random event, as a similar insertion could not be detected
469 in the short-read data of replicate transconjugants. In F048 a set of co-located
470 upregulated genes were associated with a chromosomal prophage. Many prophages
471 respond to host stress responses, which can be induced by plasmid acquisition and
472 thus may explain the upregulation of prophage gene expression observed here.

Prophages have also been shown to excise and replicate under stress conditions, but we did not detect any excision or genomic amplification of the phage region.

Besides those genes whose expression was significantly altered by ESBL plasmid acquisition (i.e. that met the stringent significance threshold), we also observed a subtle but consistent transcriptional response to plasmid acquisition among all genes with a > 2-fold change in expression. Upon acquisition of a plasmid the most intuitive scenario would be a fall in chromosomal transcription as transcriptional machinery is sequestered at plasmid promoters (Dunn et al., 2019). Accordingly, across all strains, we observed reduction in transcription of *csg* genes encoding curli fimbriae and genes involved in cell wall and outer membrane production including the *waa* LPS core genes. These genes are involved in biosynthesis of energetically costly structures in the cell and their repression is consistent with offsetting energetic costs of plasmid maintenance. Conversely, we observed consistently increased transcription of *hya, hyb, hyc* genes encoding the hydrogenase-1 and 3 complexes, the *nar* gene encoding nitrate reductase, the *ttr* gene encoding tartrate dehydratase, and the *gad* glutamate decarboxylase operon. All of these genes are involved in various aspects of anaerobic metabolism, which is known to be important for colonising the mammalian gut. Moreover, some of these genes exhibit negative frequency dependent selection in the MDR clade C of *E. coli* ST131, which may reflect selection for enhanced intestinal colonisation (McNally et al., 2019). The observation of broad-scale, subtle changes to chromosomal gene expression caused by an MDR plasmid that are consistent across diverse bacterial lineages warrants further investigation. Their scale is suggestive of a role for plasmid-encoded regulatory elements, such as small RNAs (Vial & Hommais, 2020), with the potential for genome-wide effects.

Conclusion

We observed strain-specific but limited effects of acquisition of an ESBL plasmid across diverse *E. coli* lineages. The transcriptional response to plasmid acquisition was limited to differential expression of small numbers of genes within discrete operons or regulons whose identity varied between strains. More subtle but consistent effects of plasmid acquisition on global transcription were observed, affecting a range of cellular processes. Relative growth and cefotaxime resistance of ESBL plasmid carriers varied between strains. Overall, our findings suggest that the effects of MDR plasmid acquisition upon the host cell arise from specific genetic interactions that are likely to be difficult to predict a priori and that fitness costs are unlikely to act as a barrier to plasmid transmission in natural populations of *E. coli*.

Acknowledgements

This work was funded by a BBSRC project grant [BB/R006261/1 & BB/R006253/1] jointly awarded to AM and MB respectively. We would like to thank Dr. Robert Moran for his feedback and guidance on pLL35.

Figures

Figure 1 – The level of resistance to cefotaxime conferred by the pLL35 varied by strain. Plots are facetted by *E. coli* strain. Solid lines show the mean (n=3) ± standard error of bacterial density measured using optical density (OD) at 600 nm with (red) or without (blue) pLL35 across gradients of increasing cefotaxime concentration.

Figure 2 – **The effect of acquiring pLL35 on bacterial growth kinetics varied by strain.** Panels show the response of the following growth parameters to plasmid acquisition: (A) lag time, (B) maximum growth rate, (C) maximum density, and (D) integral (i.e. area under the growth curve). Boxes show normalised values (plasmid-carrying strain value divided by parental strain value) for each strain (n=5) indicating the performance of plasmid carriers relative to their parental strain where a value of 1 represents equal performance. The lower hinge of the box denotes the 25th percentile, the upper hinge denotes the 75th percentile, and the line within the box indicates the median. Upper whiskers extend to the highest value no further than 1.5 times the inter-quartile range from the hinge. Lower whiskers extend to the smallest value no further than 1.5 times the inter-quartile range from the hinge. Points indicate outliers beyond the whiskers.

Figure 3 – **Transcriptional responses to acquiring pLL35 varied by strain.** Log_2 fold change (CTX) of differential expression data and their statistical significance (-log_{10} of the P-value). Whilst 4 of the 8 isolates showed no significant transcriptional differences, other isolates showed patterns of differential expression in discrete operons, or in genes under the control of a common regulator. The transcriptomic effects observed in this host range are determined by strain, rather than host genetic background. Blue = Significant Fold Change (>2) OR Significant P value (<0.05), Red = Also FDR Significant at a threshold of <0.10, Green = Also FDR Significant at a threshold of <0.05, Black = Not significant.

Figure 4 – **Transcriptional response of strain F022 was likely caused by a chromosomal insertion of an IS element.** A) Parental genome sequence with fully

intact lrhA gene. B) Transconjugant genome sequence with an IS1 family transposase sequence causing a truncation to lrhA. C) IS1 family transposase with left and right inverted repeat sequences, and a 9 base pair target site duplication. This particular IS1 occurs 7 times in the parental strain, and has inserted one additional time upon plasmid conjugation. Querying the ISfinder database shows that this IS1 shares 97% sequence identity with IS1 R, B and D. This element encodes two ORFs, insA and insB. D) Depth of long reads uniquely mapped to the transconjugant assembly. The minimum depth of reads that were successfully mapped to this region is 50, and in the parental isolate there are 0 reads that map to the IS1 transposase.

Figure 5 – Transcriptional change of genes from the extremes of the PCA distribution show some common signatures of differential expression (e.g. *cit* operon, *his* operon, the *hya, hyb,* and *hyc* operon, and the *nar*, *gad* and *ttd* operons). Genes were extracted from the 5th and 95th percentile of the PCA distribution from figure S6 (i.e. genes extraneous to the central distribution). These genes were assigned to COGS functional categories, with each category ordered via UPGMA clustering of the expression data.

Supplementary Material

Figure S1 – CTX-M-15 containing plasmid pLL35. A) Genomic map of pLL35 showing a complete transfer region including a full suite of conjugation machine (tra locus), and a complex antibiotic resistance region that confers resistance to cephalosporins, aminoglycosides and quinolones. Within this region, OXA-9 is found to contain a premature stop codon. pLL35 was found to contain a novel IS element flanked by a 5 bp terminal site duplication (TCCTG). B) Schematic of the resistance region, which

572 contains Tn1331b that is interrupted by a 2971 bp insertion of ISEcp1 containing a
573 1315 bp passenger section that includes CTX-M-15.
574
575 **Figure S2** – Conjugational uptake of pLL35 varied with *E. coli* strain and culturing
576 conditions. Open symbols show mean ± standard error of conjugation rate for each
577 strain and culturing condition. Colour denotes culturing condition (shaken culture =
578 green; static culture = orange). Individual replicate values are shown as different
579 symbol shapes. Symbols are jittered to prevent over-plotting.
580
581 **Figure S3** – **Stable maintenance of pLL35 in all *E. coli* strains.** Plots are facetted
582 horizontally by strain. Lines show the mean (n=4) ± standard error (shaded area)
583 bacterial population densities over time from colony forming unit counts on nutrient
584 agar plates to give the whole population (blue) or nutrient agar plates supplemented
585 with 4 µg/ml of cefotaxime to give the plasmid-carrier fraction of the population (red).
586
587 **Figure S4** – **The magnitude of the transcriptional response to pLL35 acquisition**
588 **varied by strain.** A) Number of genes that were significantly (FDR <0.05) differentially
589 expressed (>2 log fold change). B) Number of genes that were significantly (FDR
590 <0.10) differentially expressed (>2 log fold change). Red = number of genes
591 upregulated, Blue = number of genes that were downregulated.
592
593 **Figure S5** – **Global transcriptional response of ~779 core genes across all**
594 **strains, sorted by functional cog category.** Gene order is determined via UPGMA
595 clustering of log2 transcriptional changes. A = Cellular processes and signalling, B =
596 Metabolism , C = Information storage and processing, D = Poorly characterised. The

597 isolates vary in their transcriptional response to the plasmid in a strain dependent
598 manner, however a large number of metabolism genes can be seen to increase in
599 transcription across all strains. Isolate F022, belonging to ST-131 Clade A -which is
600 not typically associated with MDR plasmids – exhibits the most disparate differential
601 expression profile.
602
603 **Figure S6 – PCA distributions of expression values from functionally**
604 **categorised core genes.** A = Cellular processes and signalling, B = Metabolism , C
605 = Information storage and processing. D shows how each isolate is contributing to the
606 PCA distribution. This data highlights which genes exhibit the greatest level of
607 differential expression amongst the isolates, with several candidates in each larger
608 COG category. Panel D recapitulates the phylogenetic relatedness of isolates, with
609 environmental isolates, MDR associated and non-associated lineages appearing
610 together.
611
612 **Table S1** – Accession numbers for all read data associated with this study.
613
614 **Table S2** – Variants detected in transconjugant strains and their impact on host
615 transcription, and variants detected in independent conjugation replicates. Positions
616 highlighted in bold occur in multiple replicates.
617
618

References

Alonso-del Valle, A., León-Sampedro, R., Rodríguez-Beltrán, J., Hernández-García, M., Ruiz-Garbajosa, P., Cantón, R., San Millán, Á., Spain, M., & Peña-Miller, R. (2020). The distribution of plasmid fitness effects explains plasmid persistence in bacterial. In *bioRxiv*.

Banerjee, R., & Johnson, J. R. (2014). A New Clone Sweeps Clean: the Enigmatic Emergence of Escherichia coli Sequence Type 131. *Antimicrobial Agents and Chemotherapy*, *58*(9), 4997–5004. https://doi.org/10.1128/AAC.02824-14

Bouma, J. E., & Lenski, R. E. (1988). Evolution of a bacteria/plasmid association. *Nature*, *335*(6188), 351–352. https://doi.org/10.1038/335351a0

Brockhurst, M. A., Harrison, E., Hall, J. P. J., Richards, T., McNally, A., & MacLean, C. (2019). The Ecology and Evolution of Pangenomes. *Current Biology : CB*, *29*(20), R1094–R1103. https://doi.org/10.1016/j.cub.2019.08.012

Buckner, M. M. C., Saw, H. T. H., Osagie, R. N., McNally, A., Ricci, V., Wand, M. E., Woodford, N., Ivens, A., Webber, M. A., & Piddock, L. J. V. (2018). Clinically Relevant Plasmid-Host Interactions Indicate that Transcriptional and Not Genomic Modifications Ameliorate Fitness Costs of Klebsiella pneumoniae Carbapenemase-Carrying Plasmids. *MBio*, *9*(2). https://doi.org/10.1128/mBio.02303-17

Chilcott, G. S., & Hughes, K. T. (2000). Coupling of flagellar gene expression to flagellar assembly in Salmonella enterica serovar typhimurium and Escherichia coli. *Microbiology and Molecular Biology Reviews : MMBR*, *64*(4), 694–708. https://doi.org/10.1128/mmbr.64.4.694-708.2000

CLSI. (2012). *Methods for Dilution Antimicrobial Test for Bacteria that Grow Aerobically. M7-A*. Wayne, PA.

644 Dunn, S. J., Connor, C., & McNally, A. (2019). The evolution and transmission of
645 multi-drug resistant Escherichia coli and Klebsiella pneumoniae: the complexity
646 of clones and plasmids. In *Current Opinion in Microbiology* (Vol. 51, pp. 51–56).
647 https://doi.org/10.1016/j.mib.2019.06.004
648 Feng, Y., Liu, L., Lin, J., Ma, K., Long, H., Wei, L., Xie, Y., McNally, A., & Zong, Z.
649 (2019). Key evolutionary events in the emergence of a globally disseminated,
650 carbapenem resistant clone in the Escherichia coli ST410 lineage.
651 *Communications Biology*, *2*, 322. https://doi.org/10.1038/s42003-019-0569-1
652 Göttig, S., Riedel-Christ, S., Saleh, A., Kempf, V. A. J., & Hamprecht, A. (2016).
653 Impact of blaNDM-1 on fitness and pathogenicity of Escherichia coli and
654 Klebsiella pneumoniae. *International Journal of Antimicrobial Agents*, *47*(6),
655 430–435. https://doi.org/10.1016/j.ijantimicag.2016.02.019
656 Harrison, E., Guymer, D., Spiers, A. J., Paterson, S., & Brockhurst, M. A. (2015).
657 Parallel Compensatory Evolution Stabilizes Plasmids across the Parasitism-
658 Mutualism Continuum. *Current Biology*, *25*(15), 2034–2039.
659 https://doi.org/10.1016/j.cub.2015.06.024
660 Kottara, A., Hall, J. P. J., Harrison, E., & Brockhurst, M. A. (2018). Variable plasmid
661 fitness effects and mobile genetic element dynamics across Pseudomonas
662 species. *FEMS Microbiology Ecology*, *94*(1), 172.
663 https://doi.org/10.1093/femsec/fix172
664 Kuczyńska-Wiśnik, D., Kędzierska, S., Matuszewska, E., Lund, P., Taylor, A.,
665 Lipińska, B., & Laskowska, E. (2002). The Escherichia coli small heat-shock
666 proteins IbpA and IbpB prevent the aggregation of endogenous proteins
667 denatured in vivo during extreme heat shock. *Microbiology*.
668 https://doi.org/10.1099/00221287-148-6-1757

669 Long, D., Zhu, L. L., Du, F. L., Xiang, T. X., Wan, L. G., Wei, D. D., Zhang, W., & Liu,
670 Y. (2019). Phenotypical profile and global transcriptomic profile of Hypervirulent
671 Klebsiella pneumoniae due to carbapenemase-encoding plasmid acquisition.
672 *BMC Genomics*, *20*(1), 480. https://doi.org/10.1186/s12864-019-5705-2
673 Mahfouz, N., Ferreira, I., Beisken, S., von Haeseler, A., & Posch, A. E. (2020).
674 Large-scale assessment of antimicrobial resistance marker databases for
675 genetic phenotype prediction: a systematic review. *Journal of Antimicrobial*
676 *Chemotherapy*. https://doi.org/10.1093/jac/dkaa257
677 Mathers, A. J., Peirano, G., & Pitout, J. D. D. (2015). The role of epidemic resistance
678 plasmids and international high-risk clones in the spread of multidrug-resistant
679 Enterobacteriaceae. *Clinical Microbiology Reviews*, *28*(3), 565–591.
680 https://doi.org/10.1128/CMR.00116-14
681 McNally, A., Kallonen, T., Connor, C., Abudahab, K., Aanensen, D. M., Horner, C.,
682 Peacock, S. J., Parkhill, J., Croucher, N. J., & Corander, J. (2019).
683 Diversification of Colonization Factors in a Multidrug-Resistant Escherichia coli
684 Lineage Evolving under Negative Frequency-Dependent Selection. *MBio*, *10*(2).
685 https://doi.org/10.1128/mBio.00644-19
686 McNally, A., Oren, Y., Kelly, D., Pascoe, B., Dunn, S., Sreecharan, T., Vehkala, M.,
687 Välimäki, N., Prentice, M. B., Ashour, A., Avram, O., Pupko, T., Dobrindt, U.,
688 Literak, I., Guenther, S., Schaufler, K., Wieler, L. H., Zhiyong, Z., Sheppard, S.
689 K., … Corander, J. (2016). Combined Analysis of Variation in Core, Accessory
690 and Regulatory Genome Regions Provides a Super-Resolution View into the
691 Evolution of Bacterial Populations. *PLoS Genetics*, *12*(9), e1006280.
692 https://doi.org/10.1371/journal.pgen.1006280
693 Millan, A. S., Toll-Riera, M., Qi, Q., & MacLean, R. C. (2015). Interactions between

694 horizontally acquired genes create a fitness cost in Pseudomonas aeruginosa.
695 *Nature Communications*, *6*. https://doi.org/10.1038/ncomms7845
696 Nang, S. C., Morris, F. C., McDonald, M. J., Han, M. L., Wang, J., Strugnell, R. A.,
697 Velkov, T., & Li, J. (2018). Fitness cost of mcr-1-mediated polymyxin resistance
698 in Klebsiella pneumoniae. *Journal of Antimicrobial Chemotherapy*, *73*(6), 1604–
699 1610. https://doi.org/10.1093/jac/dky061
700 Peirano, G., Schreckenberger, P. C., & Pitout, J. D. D. (2011). Characteristics of
701 NDM-1-Producing Escherichia coli Isolates That Belong to the Successful and
702 Virulent Clone ST131. *Antimicrobial Agents and Chemotherapy*, *55*(6), 2986–
703 2988.
704 Petty, N. K., Zakour, N. L. Ben, Stanton-Cook, M., Skippington, E., Totsika, M.,
705 Forde, B. M., Phan, M. D., Moriel, D. G., Peters, K. M., Davies, M., Rogers, B.
706 A., Dougan, G., Rodriguez-Baño, J., Pascual, A., Pitout, J. D., Upton, M.,
707 Paterson, D. L., Walsh, T. R., Schembri, M. A., & Beatson, S. A. (2014). Global
708 dissemination of a multidrug resistant Escherichia coli clone. *Proc Natl Acad Sci*
709 *U S A*, *doi/10.107*.
710 San Millan, A., Toll-Riera, M., Qi, Q., Betts, A., Hopkinson, R. J., McCullagh, J., &
711 MacLean, R. C. (2018). Integrative analysis of fitness and metabolic effects of
712 plasmids in Pseudomonas aeruginosa PAO1. *The ISME Journal*, *12*(12), 3014–
713 3024. https://doi.org/10.1038/s41396-018-0224-8
714 Seemann, T. (2014). Prokka: rapid prokaryotic genome annotation. *Bioinformatics*,
715 *30*(14), 2068–2069. https://doi.org/10.1093/bioinformatics/btu153
716 Stevanin, T. M., Read, R. C., & Poole, R. K. (2007). The hmp gene encoding the
717 NO-inducible flavohaemoglobin in Escherichia coli confers a protective
718 advantage in resisting killing within macrophages, but not in vitro: Links with

719 swarming motility. *Gene*, *398*(1-2 SPEC. ISS.), 62–68.
720 https://doi.org/10.1016/j.gene.2007.03.021
721 Takahashi, Y., Shintani, M., Takase, N., Kazo, Y., Kawamura, F., Hara, H., Nishida,
722 H., Okada, K., Yamane, H., & Nojiri, H. (2015). Modulation of primary cell
723 function of host Pseudomonas bacteria by the conjugative plasmid pCAR1.
724 *Environmental Microbiology*, *17*(1), 134–155. https://doi.org/10.1111/1462-
725 2920.12515
726 Vial, L., & Hommais, F. (2020). Plasmid-chromosome cross-talks. *Environmental*
727 *Microbiology*, *22*(2), 540–556. https://doi.org/10.1111/1462-2920.14880
728 Vinué, L., Mcmurry, L. M., & Levy, S. B. (2013). The 216-bp marB gene of the
729 marRAB operon in Escherichia coli encodes a periplasmic protein which
730 reduces the transcription rate of marA. *FEMS Microbiology Letters*.
731 https://doi.org/10.1111/1574-6968.12182
732 Wick, R. R., Judd, L. M., Gorrie, C. L., & Holt, K. E. (2017). Unicycler: Resolving
733 bacterial genome assemblies from short and long sequencing reads. *PLoS*
734 *Computational Biology*, *13*(6), e1005595.
735 https://doi.org/10.1371/journal.pcbi.1005595
736 Wright, R. C. T., Friman, V.-P., Smith, M. C. M., & Brockhurst, M. A. (2018). Cross-
737 resistance is modular in bacteria-phage interactions. *PLoS Biology*, *16*(10),
738 e2006057. https://doi.org/10.1371/journal.pbio.2006057
739 Wu, W., Feng, Y., Tang, G., Qiao, F., McNally, A., & Zong, Z. (2019). NDM Metallo-
740 beta-Lactamases and Their Bacterial Producers in Health Care Settings. *Clinical*
741 *Microbiology Reviews*, *32*(2). https://doi.org/10.1128/CMR.00115-18
742 Yang, X., Ma, Q., & Wood, T. K. (2008). The R1 conjugative plasmid increases
743 Escherichia coli biofilm formation through an envelope stress response. *Applied*

and Environmental Microbiology, *74*(9), 2690–2699. https://doi.org/10.1128/AEM.02809-07

Zong, Z., Fenn, S., Connor, C., Feng, Y., & McNally, A. (2018). Complete genomic characterization of two Escherichia coli lineages responsible for a cluster of carbapenem-resistant infections in a Chinese hospital. *Journal of Antimicrobial Chemotherapy*, *73*(9), 2340–2346. https://doi.org/10.1093/jac/dky210

751

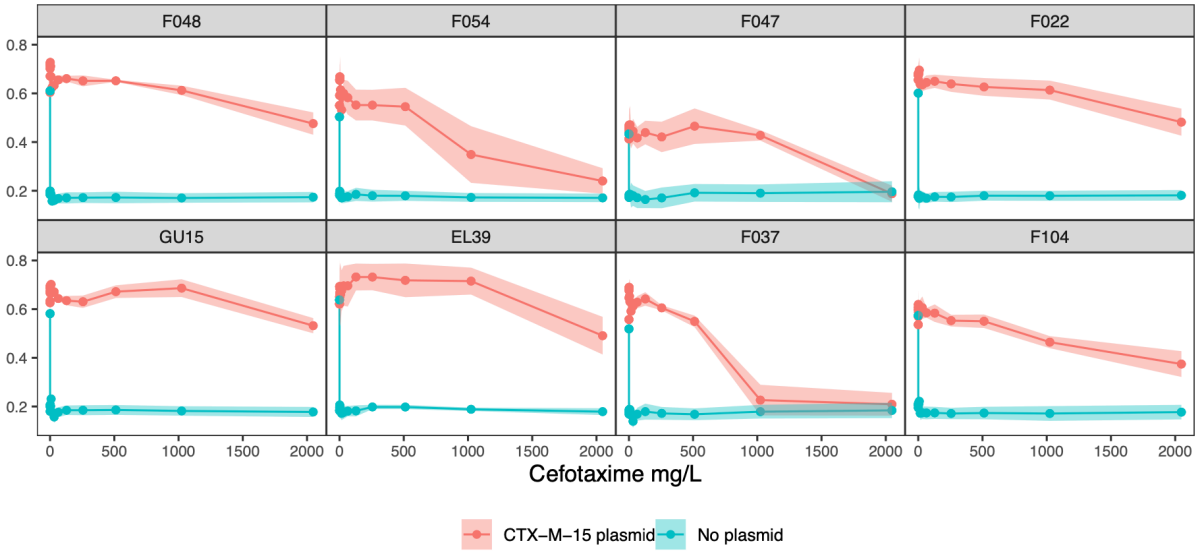

752

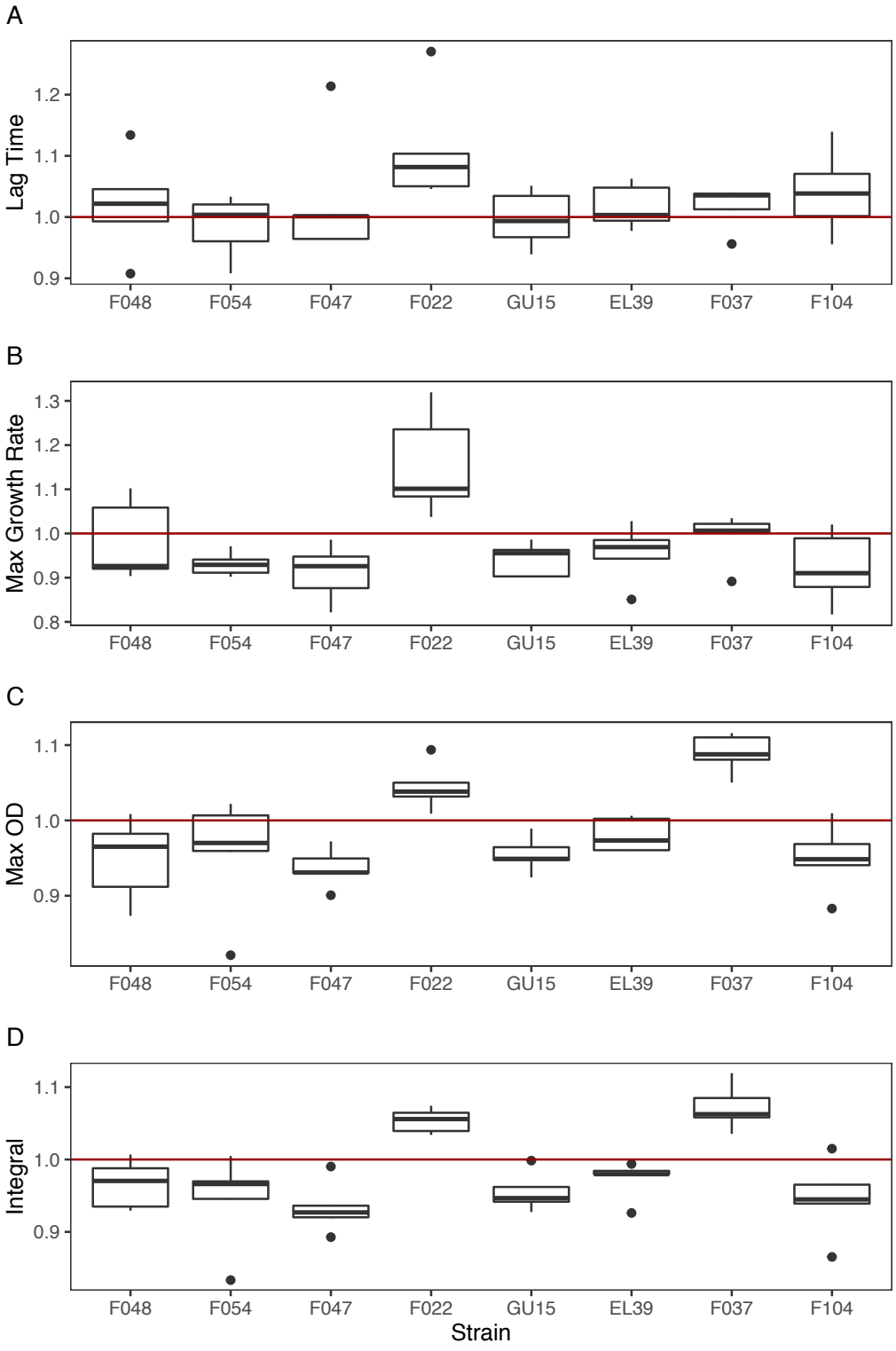

753

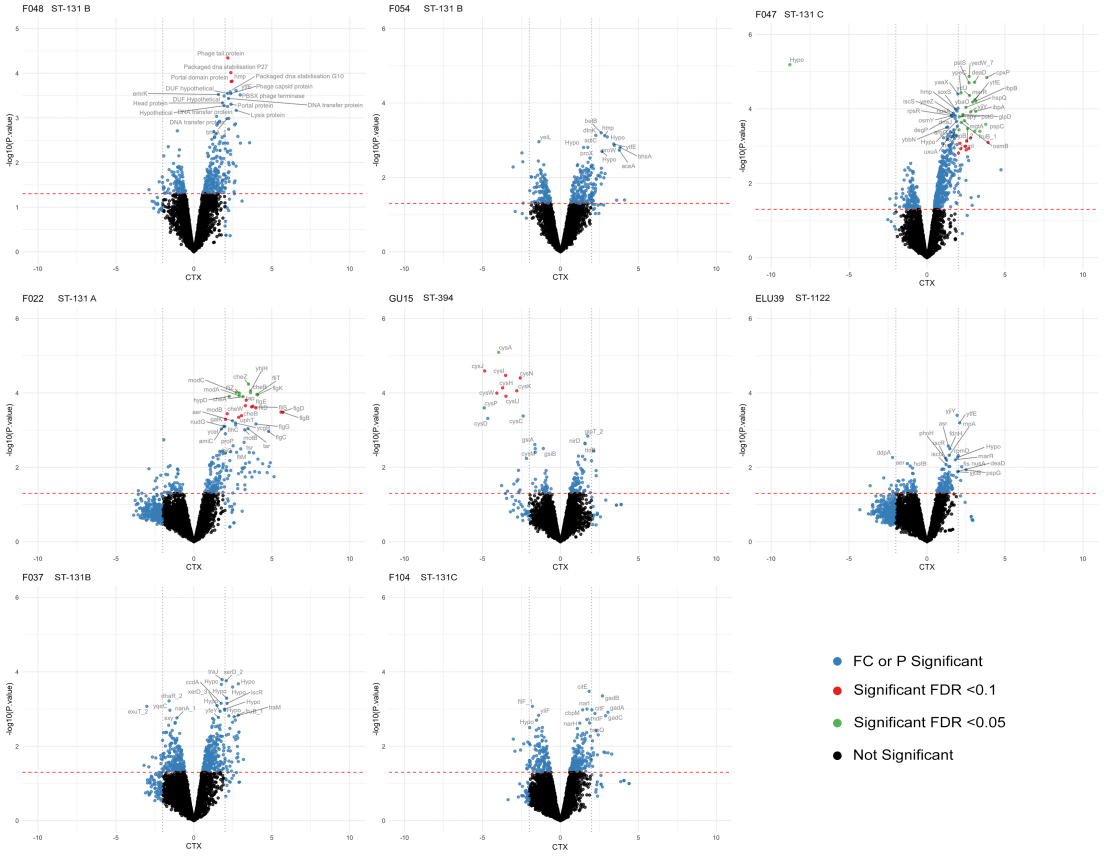

754